32 Berrettini, W. H. *et al.* (1988) *Neuropsychobiology* 19, 64–68
33 Beal, M. F. *et al.* (1988) *J. Neurochem.* 51, 1935–1941
34 Hökfelt, T. *et al.* (1987) *Experientia* 43, 768–780
35 Agid, Y., Javoy, F. and Glowinski, J. (1983) *Nature* 245, 150–151
36 Bartfai, T., Iverfeldt, K. and Fisone, G. (1988) *Annu. Rev. Pharmacol. Toxicol.* 28, 285–310
37 Hardy, J. *et al.* (1985) *Neurochem. Int.* 7, 545–563
38 Dunnett, S. B., Whishaw, I. Q., Jones, G. H. and Bunch, S. T. (1987) *Neuroscience* 20, 653–669
39 Wenk, G. L., Markowska, A. and Olton, S. D. *Behav. Neurosci.* (in press)
40 Gabriel, S. M. *et al.* (1988) *Neurosci. Lett.* 87, 114–120
41 Amiranoff, B., Lorinet, A. M., Yanaihara, N. and Laburthe, M. (1989) *Eur. J. Pharmacol.* 163, 205–207
42 Fox, J. E. T. *et al.* (1988) *Peptides* 9, 1183–1189
43 Rökaeus, Å. and Brownstein, M. J. (1986) *Proc. Natl Acad. Sci. USA* 83, 6287–6291
44 Kaplan, L. M., Spindel, E. R., Isselbacher, K. J. and Chin, W. W. (1988) *Proc. Natl Acad. Sci. USA* 85, 1065–1069
45 Vrontakis, M. E., Peden, L. M., Duckworth, M. L. and Friesen, H. G. (1988) *J. Biol. Chem.* 262, 16755–16758
46 Rökaeus, Å. and Carlquist, M. (1988) *FEBS Lett.* 234, 400–406

techniques

In vivo *functional localization of the human visual cortex using positron emission tomography and magnetic resonance imaging*

Bassem N. Mora, George J. Carman and John M. Allman

Bassem N. Mora, George J. Carman and John M. Allman are at the Division of Biology 216–76, California Institute of Technology, Pasadena, CA 91125, USA.

Positron emission tomography (PET) and magnetic resonance imaging (MRI) are two recently developed methods for imaging the human brain in vivo. One application of PET measures stimulus-evoked changes in cerebral blood flow while MRI provides a detailed anatomical map of the brain. Here we report the combined application of these two techniques in the same human subject. Subtracted PET scans of a brain receiving visual stimulation were superimposed upon MRI images of the same brain. The PET scans were converted into the MRI coordinate space before superposition, which allowed for a more precise correlation between MRI anatomical data and PET physiological data. Responses were localized in striate and extrastriate visual areas as well as in the posterior thalamus.

The application of physiological and anatomical techniques[1–3] has led to the discovery in non-human primates of a large number of cortical visual areas, some of which have definite functional specializations. Knowledge of the organization of human visual cortex has been mainly limited to the inferences gained from the observation of patients afflicted by brain injuries[4–6]. However, the advent of new brain imaging techniques has made it possible to study experimentally the organization of human visual cortex. Stimulus-evoked changes in regional cerebral blood flow (rCBF) monitored with positron emission tomography (PET) can be used to investigate the physiological responses of the brain. The anatomical structure of the brain can be obtained by proton nuclear magnetic resonance imaging (MRI). In this study, we have sought to combine the physiological-localizing ability of PET with the anatomical-resolving power of MRI in parallel observations made in the brain of the same subject.

PET measures local concentrations of positron-emitting compounds injected into living tissue. Cortical blood flow is measured by monitoring changes in the concentration of water labeled with oxygen-15 ($H_2{}^{15}O$) in the brain. Increases in neural activity within a brain region lead to increases in rCBF in that region[7–9]. Recently, the retinotopic organization of primary visual cortex has been mapped in normal human volunteers using stimulus-evoked changes in rCBF[10]. This was accomplished by first obtaining a control PET scan, where the subject is looking at a small fixation point on a computer screen. This control scan measures background brain activity. The presentation of different stimuli on the computer screen then activates cortical areas, which leads to increased rCBF, which is detected by PET. The stimulus PET scan therefore contains background brain activity in addition to cortical activity due to the stimulus. Subtraction of the control from the stimulus PET scans results in a map of cortical activity due to the visual stimulus[11].

The PET scans used in this study were performed at Washington University School of Medicine, MI, USA, by Raichle, Fox, Miezin, Allman and co-workers. The PETT VI system was used, which simultaneously acquires seven parallel horizontal brain slices[12]. Each horizontal slice consisted of a 100 × 100 matrix of measurements (2.7 mm × 2.7 mm) with an interslice center-to-center distance of 14.4 mm. The effects of global CBF fluctuations on each of the seven horizontal PET scans were minimized by normalizing the images such that the total brain blood flow was 50 ml per 100 g per min, as described elsewhere[11,13].

After performing the fixation-point control PET scan, a stimulus was presented on the computer screen, and the stimulus scan was taken. This sequence of control/stimulus scans was repeated four times, once for each of the four stimuli that were used. All stimuli consisted of a red and black checkerboard annulus with a central fixating point and varying eccentricities. The red and black checks alternated at a frequency of 10 Hz in order to maximize the induced CBF responses[8]. The stimuli were: a *macular* annulus, extending radially from 0.1° to 1.5°, with a radial check size of 0.5°; a *peri-macular* annulus, ranging from 1.5° to 5.5°, with a radial check size of 1.0°; and *peripheral* hemi-annuli, extending from 5.5° to 15.5°, one *upper-field* and the other *lower-field*, with a radial check size of 2.0°.

MRI is a technique developed during the past

0166 - 2236/89/$03.50

decade to provide high-resolution anatomical images of living tissue by recording the mobility of protons. It provides a high level of contrast between gray and white matter. The MRI images used in this study, taken of the same subject at an earlier date, were obtained using a Diasonics 0.35 T scanner at the Huntington Medical Research Institutes, CA, USA. The images were obtained in the coronal and parasagittal planes using the spin-echo technique with a relaxation time, T_r, of 3 s and an echo time, T_e of 100 ms[14]. The parasagittal images were used for PET–MRI superpositioning, with an in-plane resolution of 0.95 mm and a slice thickness of 2.7 mm. After transfer to a Masscomp 5700 computer, each 256 × 256 pixel MRI image was expanded by linear interpolation in each of two orthogonal directions in the image plane to yield a 768 × 768 pixel image.

The alignment of the PET slices with respect to cranial features was determined from a lateral X-ray radiograph taken at the time of the PET scan with the subject's head held in a fixed position relative to the scanner. The radiograph in the upper-left panel of Fig. 1 shows the outline of the skull in the mid-sagittal plane with the centers of the seven horizontal PET slices. The radiograph was superimposed on the mid-sagittal MRI to align the PET and MRI coordinate systems. This resulted in the PET–MRI superpositions shown in Fig. 1, with the PET scans displayed as a transparent overlay in register with the MRI images. The scale used in the displays is illustrated at the top of Fig. 1, with MRI image intensity increasing to the right, and PET image intensity increasing to the bottom. Maximum PET response is in red to allow easier localization of the response focus. The upper-right panel of Fig. 1 depicts the cortical response to macular stimulation *without* subtraction of the fixation-point control scan. The bottom four panels of Fig. 1 illustrate the *net* responses to macular, perimacular, lower- and upper-field stimulation after the subtraction of the matching fixation-point control scans. They are all displayed using the same intensity scale. In the center-left panel, the macular stimulus produced a focal response at the posterior tip of the calcarine sulcus. The perimacular stimulus produced a response centered immediately anterior to the macular stimulus (center-right panel). The lower-field peripheral stimulus produced a response centered in the upper bank of the calcarine sulcus (lower-left panel), while the upper-field peripheral stimulus produced a response centered in the lower bank of the calcarine sulcus (lower-right panel). Changing the portion of the visual field being stimulated therefore shifts the PET response locales in visual cortex. The visuotopic organization thus revealed closely matches that inferred from visual-field defects produced by restricted visual-cortex lesions in humans[4–6].

Figure 2 shows the net responses to macular stimulation obtained from the extrastriate cortex and posterior thalamus in the same subject. The

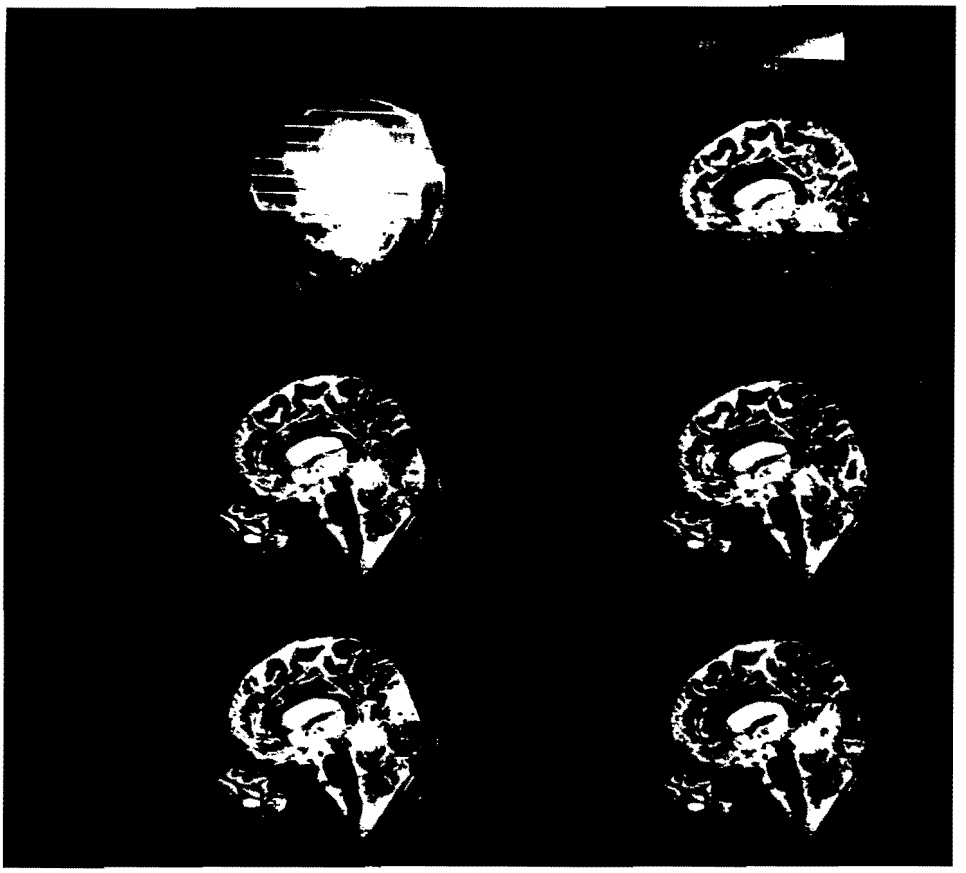

Fig. 1. *PET–MRI superimposed images from the same subject, showing cortical responses due to visual cortex stimulation.* Top left: *X-ray radiograph of the subject's head in the mid-sagittal plane with the centers of the seven horizontal PET planes delineated, plane 1 being the top-most plane and plane 7 the bottom-most plane. The remaining images are PET–MRI superimposed images localizing physiology on to anatomy. Shown to the left of each PET–MRI subtracted image is the stimulus used to activate the corresponding cortical structures. Shown at the top is the two-dimensional linear scale used in the display of the images: the horizontal axis is used to represent the MRI data, with MRI image intensity increasing horizontally to the right; the vertical axis is used to represent the PET data, with PET image intensity increasing vertically downwards. Thus, points in the superimposed images that have maximal PET activity and maximal MRI signal are represented in the bottom-right of the scale. The red in the PET scale allows easier localization of the peak PET responses in the images.* Top right: *cortical response to macular stimulation without subtraction of the control scan.* Center left: *subtracted response to macular stimulation following subtraction of the control scan.* Center right: *subtracted response to perimacular stimulation.* Bottom left: *subtracted response to peripheral lower-field hemi-annulus stimulation.* Bottom right: *subtracted response to peripheral upper-field hemi-annulus stimulation.*

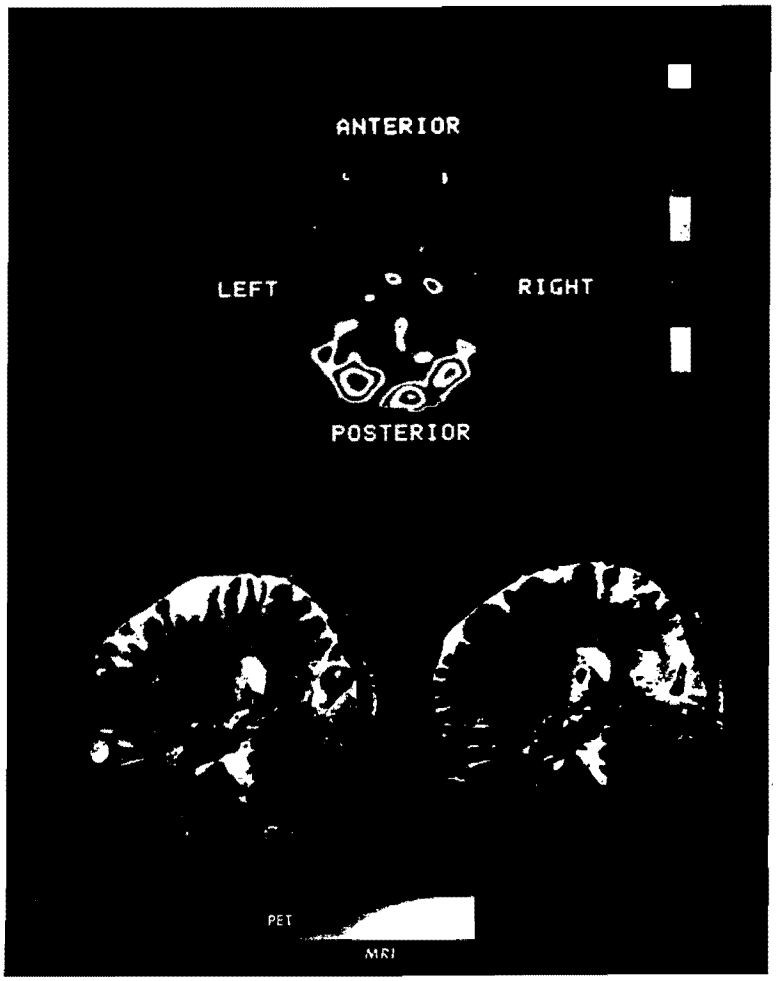

Fig. 2. *Subtracted responses to macular stimulation in extrastriate cortex and posterior thalamus in the same subject.* Top panel: *Conventional display of the subtracted response from horizontal PET plane 6.* Bottom panel: *parasagittal PET–MRI images illustrating subtracted cortical response at 2 cm from the midline. Right and left panels correspond to the right and left hemispheres of the brain, respectively. Note the activation of extrastriate visual cortex and the posterior region of the thalamus, which are more clearly observed using PET–MRI superpositioning (bottom) compared with a conventional PET display (top). The scale used in this display was different from that used in Fig. 1.*

upper portion is the response from horizontal PET plane six showing a peak centered on the midline, which intersects with the peak illustrated in the center-left panel of Fig. 1. The lower panels of Fig. 2 are parasagittal images, 2 cm to the left and right of the midline, which contain approximately symmetrical responses in the extrastriate visual cortex. These lateral extrastriate zones probably include the temporal-occipital-parietal pit (TOPP), which in other subjects was found to respond to fast-flickering and low-contrast, moving dot patterns and may correspond to area MT[15–17]. There are also responses in the posterior thalamus, which may arise in part from the lateral geniculate nucleus but appear to be centered more dorsally in the pulvinar complex. In monkeys, the pulvinar contains several maps of the visual field, in a manner analogous to the visual areas in extrastriate cortex[18,19].

PET–MRI superposition permits the observation of physiological responses displayed in register with brain structures from the same individual. This contrasts with the standard localization method used in PET studies in which averaged data from different subjects are referred to coordinates in a stereotactic atlas[13]. This method of referring PET data to a standard atlas is valuable but suffers from the difficulties presented by the substantial inter-subject variability among human subjects[20–22]. This problem of variability may be particularly acute in extrastriate cortex where the responses are lower in amplitude and the size of the constituent areas may be smaller than in primary visual cortex.

Selected references

1 Allman, J. M. and McGuinness, E. R. (1988) in *Comparative Primate Biology, Vol. 4: The Neurosciences* (Steklis, H. D. and Erwin, J., eds), pp. 279–326, Alan R. Liss
2 Van Essen, D. C. (1985) in *Cerebral Cortex* (Vol. 3) (Peters, A. and Jones, E. G., eds), pp. 259–329, Plenum Press
3 Zeki, S. M. (1978) *Nature* 274, 423–428
4 Inouye, T. (1909) *Die Sehstörungen bei Schussverletzungen der kortikalen Sehsphäre nach Beobachtungen an Versundeten der letzten Japanische Kriege* W. Engelmann
5 Holmes, G. and Lister, W. T. (1916) *Brain* 39, 34–73
6 Teuber, H., Battersby, W. and Bender, M. (1960) *Visual Field Deficits after Penetrating Missile Wounds* Harvard University Press
7 Brodersen, P. *et al.* (1973) *Arch. Neurol.* 28, 334–338
8 Fox, P. T. and Raichle, M. E. (1984) *J. Neurophysiol.* 51, 1109–1120
9 Paulson, O. B. and Newman, E. A. (1987) *Science* 237, 896–898
10 Fox, P. T. *et al.* (1986) *Nature* 323, 806–809
11 Fox, P. T., Miezin, F. M., Allman, J. M., Van Essen, D. C. and Raichle, M. E. (1987) *J. Neurosci.* 7, 913–922
12 Yamamoto, M., Ficke, D. C. and Ter-Pogossian, M. M. (1982) *IEEE Trans. Nucl. Sci.* 29, 529–533
13 Fox, P. T., Perlmutter, J. S. and Raichle, M. E. (1985) *J. Comp. Ass. Tomog.* 9, 141–153
14 Bradley, W. G., Newton, T. H. and Crooks, L. E. (1983) in *Modern Neuroradiology, Vol. 2: Advanced Imaging Techniques* (Newton, T. H. and Potts, D. G., eds), pp. 15–61, Claradel Press
15 Allman, J. (1988) in *Visual Processing of Form and Motion* (Rauschecker, J. and Mohn, G., eds), pp. 33–34, Tübingen
16 Miezin, F. M., Fox, P. T., Raichle, M. E. and Allman, J. M. (1987) *Soc. Neurosci. Abstr.* 13, 631
17 Miezin, F. M., Fox, P. T., Raichle, M. E. and Allman, J. M. (1988) *ARVO Abstr.* p. 326
18 Allman, J. M., Kaas, J. H., Lane, R. H. and Miezin, F. M. (1972) *Brain Res.* 40, 291–302
19 Bender, D. B. (1981) *J. Neurophysiol.* 46, 672–693
20 Talairach, J. and Szikla, G. (1967) *Atlas d'Anatomie Stereotaxique du Telencephale* Masson
21 Schaltenbrand, G. and Bailey, P. (1959) *Introduction to Stereotaxis with an Atlas of the Human Brain* Thieme
22 Stensaas, S. S., Eddington, D. K. and Dobelle, W. H. (1974) *J. Neurosurg.* 40, 747

Acknowledgements

We thank Marcus Raichle, Peter Fox, Fran Miezin, Joel Perlmutter and Tom Videen at Washington University School of Medicine in St Louis for their time and effort in performing the PET scans, and for generously offering technical advice and assistance, David Van Essen of the California Institute of Technology for his interest in this project and for use of his computer laboratory, and William Bradley of the Huntington Medical Research Institutes for providing the MRI images. This work has been supported by grants from NIH, the Gordon Trust, the Sloan Foundation, and the McDonnell Center for Higher Brain Research. Part of the equipment used in this project was acquired through support from Office of Naval Research contract number N0014-85K-0068 to D. Van Essen.